Investigation of MR-FBP method and comparisons with ASTRA algorithms and a deep learning approach

Kyriakos Aristidou (s3510123)
Antonia Christodoulou (s3614794)

***Abstract*—This paper aims to evaluate the MR-FBP performance by investigating several scenarios and even comparing it with deep neural networks. More specifically, we run certain experiments which aim to give a better understanding of the weak and strong points of the method and conclude certain cases when MR-FBP could outperform other already existing algorithms. Some scenarios that we examine is the performance of the method on different types of phantoms, its performance compared to other algorithms provided by the ASTRA toolbox, angle limitations, and noise additions. Finally, we build and implement a simple CNN to make even more comparisons with our algorithm. Eventually, we come to the conclusion that MR-FBP is indeed easy and simple to use algorithm, not very complex which is suitable for simpler setups when the image is not very complicated and we can have access to the full angle range of the object. When it comes to the deep learning approach, using a CNN might give more accurate reconstructions but it requires special training on each phantom. In another case, it does not perform well and our algorithm, MR-FBP is preferable.**

***Index Terms*—tomography, image reconstruction, MR-FBP, ASTRA toolbox, data-dependent filtering, CNN, deep learning.**

I. Introduction

This paper presents a comprehensive investigation of the Minimum Residual Filtered Backprojection (MR-FBP) algorithm for tomographic image reconstruction and an attempt to compare this algorithm with other reconstruction algorithms using ASTRA library and with a deep learning approach. The MR-FBP algorithm, introduced by Pelt and Batenburg [1], offers a novel approach that incorporates data-dependent filtering to enhance the accuracy and processing efficiency of filtered backprojection reconstruction.

The paper presents a series of experiments to evaluate the performance and effectiveness of the MR-FBP algorithm in various contexts. These experiments involve applying MR-FBP to phantoms with various characteristics, contrasting MR-FBP with popular algorithms, analyzing the effects of various angle ranges on reconstruction, examining the impact of noise on reconstruction quality, and investigating how well MR-FBP performs in comparison to a deep learning method utilizing a convolutional neural network.

The experiments aim to evaluate the MR-FBP algorithm's performance in reconstructing various phantom types, compare it to other reconstruction algorithms, examine the impact of angle restrictions and noise on reconstruction quality, and assess how well it competes with deep learning techniques. The outcomes of those experiments will be covered in more detail later on in the paper.

The paper consists of several sections that explore different aspects of the MR-FBP algorithm and its application in tomographic image reconstruction. These sections include the methodological details of the MR-FBP algorithm, a series of experiments to evaluate its performance and a comparison with other algorithms, an analysis of the test data used in the experiments, a description of the experimental setup, an overview of the results obtained from the experiments, and a discussion of the findings and conclusions.

II. Method

The MR-FBP algorithm provides a reconstruction method with a data-dependent filter that improves accuracy and processing efficiency by combining concepts from analytical and algebraic approaches. The following subsections are the main steps of the MR-FBP algorithm

A. Calculation of the Linear Operator

The FBP algorithm, which is a linear operation on the projection data, can be represented as a linear operator $\mathcal{M} : \mathbb{R}^{N_d N_\theta} \to \mathbb{R}^{N^2}$. This operator is applied to the projection data p and can be represented by this equation:

$$\mathrm{FBP}_{\boldsymbol{h}}(\boldsymbol{p}) = \boldsymbol{M_h p} \tag{1}$$

B. Optimization of Data-Dependent Filter

The MR-FBP algorithm improves upon the standard FBP method by replacing the standard filter h with a specific data-dependent filter, denoted as h^*. This filter is obtained by minimizing the squared difference between the projections of the reconstruction and the measured projection data, as expressed in equation (2). By solving the least squares problem stated in equation (3), with $A_p = WW^T C_p$, the optimized filter h^* is computed.

$$h^* = \underset{h}{\operatorname{argmin}} \left[p - W\,\mathrm{FBP}_h(p)\right]^2 \tag{2}$$

$$A_p h = p \tag{3}$$

C. MR-FBP Reconstruction

The MR-FBP reconstruction is obtained by performing filtered backprojection using the optimized filter h^*. This involves convolving the projection data p with the filter h^*, as described in equation (11) in [1]. The resulting filtered projections are backprojected to generate the final reconstructed image.

The complete MR-FBP algorithm can be summarized using the following pseudocode which is taken from the paper [1]:

Algorithm 1 MR-FBP reconstruction method

1: Calculate $A_p = WW^T C_p$
2: Find the least squares solution h^* of $A_p h = p$
3: Return $FBP_{h^*}(p)$ as the MR-FBP reconstruction

The benefits of the MR-FBP approach include higher precision for challenges with sparse data and computational efficiency. The MR-FBP algorithm improves the quality of the reconstructed images by including a data-dependent filter and making use of the filtered backprojection principles. More details about the algorithm are presented in the official paper [1].

III. Experiments

In this section, we will describe all of our experiments making our goals clear as well as which subquestions we aim to answer by each experiment. Eventually, you will gain an idea of how our work is structured.

A. Experiment 1: Implementing MR-FBP on phantoms with different properties.

The goal of the first experiment is to implement the MR-FBP method on phantoms with varying characteristics. The purpose of this study is to assess the effectiveness of the MR-FBP reconstruction technique on a variety of phantoms.

More specifically, we want to examine and compare the quality of the reconstruction obtained by MR-FBP when dealing with the following groups of phantoms (as we have grouped them based on specific characteristics):

- more simple basic grayscale phantoms
- binary (black and white) phantoms
- clinical phantoms (brain-like)
- continuous phantoms

So, with this experiment, we come to answer the question of how does the algorithm perform? Does it give high-quality reconstructions? Is its usage easy and user-friendly? How does its performance be affected by different characteristics of the phantoms? Does it work better on a specific group instead of another? By evaluating the reconstructed images obtained from the MR-FBP algorithm, we can gain insights into its suitability and sufficiency for different types of tomographic imaging scenarios.

B. Experiment 2: Comparing MR-FBP with commonly used algorithms.

The goal of this experiment is to compare the performance of the MR-FBP algorithm to the performance of other commonly used reconstruction algorithms, such as FBP (Filtered BackProjection), SIRT (Simultaneous Iterative Reconstruction Technique), SART (Simultaneous Algebraic Reconstruction Technique), and CGLS (Conjugate Gradient Least Squares). The goal is to assess and compare the quality of reconstruction and validity of various algorithms for tomographic image reconstruction.

But first, here are a few words for each of the above algorithms so that we can have a main idea of how they work and how they differ from MR-FBP:

- **MR-FBP:** MR-FBP stands for Minimum Residual Filtered Backprojection and it is a reconstruction algorithm that combines the principles of filtered backprojection (FBP) with iterative optimization techniques to improve the quality of the reconstructed images[1]. The reconstruction method in MR-FBP entails minimizing the residual error between the collected projection data and the predicted projections from a given image estimate iteratively. This iterative optimization aids in reconstruction improvement by iteratively updating the image approximation to reduce the error between measured and estimated data.

- **FBP:** Filtered Back Projection (FBP) is a popular tomographic image reconstruction approach. It works by first performing a Fourier domain filtering operation on the collected projection data. This filtering process is designed to improve image quality and reduce noise. FBP reconstructs the image via back projection after obtaining the filtered projections.
  However, FBP has some disadvantages that MR-FBP aims to minimize. FBP assumes a linear imaging system and ignores the imaging system's non-uniform frequency response. This can result in visual effects (artifacts) and poor accuracy, especially when there is noise or missing data. Although FBP is computationally efficient and allows rapid reconstruction, it may not provide excellent image quality in difficult conditions so it is interesting to compare it with MR-FBP.

- **SIRT:** SIRT (Simultaneous Iterative Reconstruction Technique) is a tomographic image reconstruction iterative algorithm. It handles the reconstruction problem by iteratively updating the image estimate to minimize the difference between the acquired and estimated projection data. SIRT is based on an algebraic reconstruction technique, in which the reconstruction challenge is presented as a system of linear equations. It iteratively adjusts the picture estimation by taking forward and backward projection inconsistencies into account. SIRT considers the differences between the acquired and projected projection data throughout each cycle and uses this information to refine the image estimate. However, it is important to consider that SIRT can be computationally demanding (unlike MR-FBP), especially for large-scale tomographic reconstructions. The number of iterations required for convergence can

also affect the computational time.

- **SART:** SART is an iterative technique extensively used for tomographic image reconstruction. It combines features of algebraic reconstruction techniques with tactics for simultaneous updating.
  SART updates the image estimate iteratively based on the algebraic equations that characterize the imaging process. SART, unlike some other iterative algorithms, considers many projections at the same time during each iteration, hence the term "simultaneous" in its name. SART is able to establish a compromise between reconstruction accuracy and computational cost because of this simultaneous updating technique.
  While both SART and MR-FBP are iterative algorithms, they differ in terms of optimization methodologies and unique imaging system requirements. SART emphasizes multiple updates and algebraic reconstruction, whereas MR-FBP integrates iterative optimization.

- **CGLS:** Conjugate Gradient Least Squares (CGLS) is a tomographic image reconstruction iterative technique. It approaches the reconstruction problem as a least-squares optimization framework.
  The conjugate gradient approach is used by CGLS to repeatedly minimize the difference between the collected projection data and the projected projections. The conjugate gradient method is an optimization approach that solves linear systems of equations effectively. CGLS uses the conjugate gradient method in the context of tomographic reconstruction to repeatedly update the image estimate and find out the solution that best fits the collected projection data. However, CGLS can, also, be computationally demanding, especially for large-scale tomographic reconstructions.

So, here we compare the performance of MR-FBP with algorithms that might claim to give more accurate reconstructions but are computationally expensive and algorithms that might be faster but not give so high-quality images. In the end, after implementing all those algorithms, we will discuss if MR-FBP could be preferable under certain circumstances or if it is worth sacrificing quality for computational time and conclude with some overall comparisons.

C. *Experiment 3: Angles limitation.*

In this experiment, we want to examine how different angle ranges affect tomographic image reconstruction. We concentrated on four different angle configurations in particular: [0, π], [0, π/2], [0,π/4], and [0,π/8]. Of course, we could, also, examine more angle ranges but we consider these four to be representative enough. So, here we want to see how changing the range of angles affects the quality and accuracy of the reconstructed images.

In general, the quantity and distribution of obtained projections around the object being captured are determined by the angle configurations used in tomographic imaging. A larger angle range, such as [0,π], provides a complete set of projections that wraps around the object 180 degrees. A tighter angle range, such as [0,π/8], on the other hand, captures just a limited angular range, resulting in sparse projection data.

So, angle limitations can have a substantial impact on reconstruction. With a broader angle range, the obtained projections provide detailed information about the attenuation qualities of the object from various viewing angles. This results in increased reconstruction accuracy, higher spatial resolution, and fewer artifacts. However, due to equipment or time limitations, capturing a full range of projections may not always be possible in some circumstances.

A narrower angle range, on the other hand, captures fewer projections, resulting in an incomplete sampling of the object's attenuation information. This can result in poor image quality, increased noise, and artifacts. Sparse angle sampling might make it difficult to estimate the object's features accurately, resulting in blurring or noise of the reconstructed images.

We can analyze the impact of angle limitations on the quality of the image, spatial resolution, and overall reconstruction performance by comparing the reconstruction results obtained from the four angle configurations. This study offers an understanding of the trade-off between obtaining a complete set of projections with a greater angle range and a limited angular sampling strategy. Understanding the impacts of angle limitations can help guide the improvement of data acquisition techniques in tomographic imaging, allowing for a better balance of imaging requirements and practical constraints.

D. *Experiment 4: Noise effect.*

In this series of experiments, we aim to investigate the impact of noise in tomographic image reconstruction. We explored three different scenarios to understand how noise affects the reconstructed images: adding noise to phantoms, adding noise to sinograms, and removing noise from sinograms when dealing with limited angles.

*1) **Adding noise to phantoms**:* Firstly, we add noise from normal distribution or gaussian filter to some of the phantoms (the brain-like phantom and the continuous phantom) before reconstructing them. We replicated the influence of noise on the object being projected by directly introducing noise to the phantoms. This experiment allowed us to investigate how noise affects the accuracy, detail retention, and overall image quality of reconstructed images.

*2) **Adding noise to sinograms**:* Before completing the reconstruction, we introduced synthetic noise to the obtained sinograms. Sinograms represent projection data obtained from various angles. We simulated noise in the obtained data by inserting noise into the sinograms, which could be caused by detector noise, noise from the electrical system, or statistical noise. With this experiment, we were able to explore how noise in the input data impacts the reconstruction process, including accuracy, noise propagation, and the capacity to

retrieve small details in the reconstructed images.

3) ***Disabling noise addition from sinograms when dealing with limited angles****:* As previously explained, we made some experiments with tighter angle range which, as you will observe in the Results section, gave terrible results. The addition of noise to the sinogram before the reconstruction is something that can be turned off if the user wants to. So, using the reconstruction function that we build, we turned off the addition of noise to sinograms when dealing with phantoms captured by a limited angle range to examine if, now, the reconstructed image is more accurate. The results and discussion will be presented in the Results section.

E. ***Experiment 5: Deep Learning Approach.***

Finally, we introduced a deep learning approach where we build a Convolutional Neural Network (will be described in the Experimental Setup section) aiming to investigate if MR-FBP can compete even a neural network. Does MR-FBP give higher quality recosntructions than neural network? If yes, does this hold only in specific scenarios? All these will be presented and discussed in the following sections.

IV. Test data

As aforementioned, we use four types of phantoms and we group them as follows. The specific images are taken by setting specific values to certain variables such as the radius, the size, the margins but these are just examples and variations of the following phantoms can be reproduced using different values of the variables of each phantom generator.

A. ***Binary Phantoms.***

To begin with, we use a simple black-and-white phantom constructed using NumPy arrays and representing a simple pattern. The aim behind this phantom is to begin with something simpler to rebuild, less complex, and free of noise. In *Figure 1*, you can see an example obtained by our binary phantom generator.

B. ***Grayscale Phantoms.***

Moving forward, the phantom is again utilizing Numpy arrays to generate many different forms (two triangles, one circle and one thick line), some of which may be overlapping but now colored in different gray tones (some lighter and others darker). The background is completely black. *Figure 2* shows an example of what such a phantom looks like. The shapes sizes and tones can be modified using our generator for grayscale phantoms.

C. ***Clinical-based Phantoms.***

The following phantom resembles a human brain which makes it ideal to examine clinical cases and how MR-FBP can deal with more complex structures. So, once again, we used Numpy arrays to build various forms in an attempt to emulate the human brain. Finally, we added noise from the normal distribution with m=0 and sd=0.05 to make reconstruction more difficult.

Fig. 1: Binary (black and white) Phantom built by NumPy arrays without added noise.

Fig. 2: Grayscale phantom built by NumPy arrays.

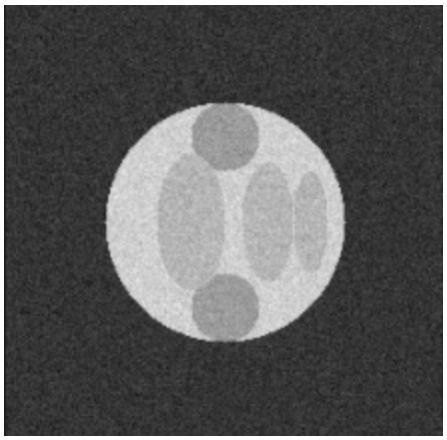

Fig. 3: Phantom based on clinical images representing a human brain with added noise from the Normal distribution.

D. ***Continuous Phantoms.***

Finally, we created a continuous phantom generator, that begins brighter at a specific point and gets darker as you get further ending with a black background. The shapes consisting this phantom is an ellipse, two circle and a square. Also, we added a Gaussian filter to the square and one of the circle with parameter sigma=2 to get a more blurred image and examine how the algorithm will perform under these circumstances.

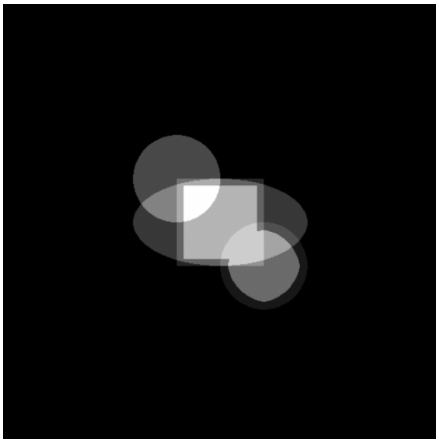

Fig. 4: Continuous blurry phantom with Gaussian noise.

V. Experimental setup

In this section, we introduce the steps that were performed for all the experiments. It is worth mentioning that the parameters used for the reconstruction algorithm, such as the number of iterations and noise level, were kept constant to ensure a fair comparison among the algorithms.

Through these experiments, we aim to compare the performance of the MR-FBP algorithm with other commonly used reconstruction algorithms and evaluate their effectiveness in producing accurate reconstructions for different types of phantoms. The evaluation based on mean absolute pixel errors will provide insights into the effectiveness of each algorithm and its suitability for various imaging scenarios.

A. Data Acquisition and Phantom Generation

The phantoms were created and prepared as input for the reconstruction algorithms. Using ASTRA library we utilized and create the necessary geometries for the reconstruction. Specifically, a volume geometry of size 256x256 was created, along with a parallel projection geometry having the option to use an angular range from 0 to π and 32 projection angles.

B. Sinograms and Reconstruction

The forward projection of each phantom was calculated using the created projector. The resulting sinograms were obtained and stored. Optionally, noise was added to each sinogram using a function from ASTRA, with a noise level of 10^4. The images were reconstructed using the reconstruction algorithms, with 200 iterations applied to each reconstruction.

C. Visualization and Evaluation

A 2x2 grid of subplots was created using matplotlib library. Each subplot displayed a specific reconstructed image corresponding to a particular phantom or reconstruction algorithm according to the experiment. The mean absolute pixel error was calculated for each reconstructed image by comparing it with the ground truth phantom image and reported for each reconstructed image.

D. Deep Learning approach

In addition to the traditional reconstruction algorithms, we also explore the application of a deep learning approach for tomographic image reconstruction. This subsection outlines the specific steps involved in training and evaluating a deep learning model for comparison with the MR-FBP and other aforementioned reconstruction algorithms. We employ a deep learning approach inspired by the U-Net architecture for tomographic image reconstruction. The U-Net is a popular neural network model that has demonstrated excellent performance in various image segmentation and reconstruction tasks.

The procedure starts with defining the model, which consists of an encoder and a decoder. The encoder is in charge of obtaining relevant data from the input sinogram, while the decoder aims to reconstruct the image using the extracted features. The encoder consists of 2 convolutional layers followed by non-linear activation functions ReLU, to capture complex patterns and structures. The decoder comprises transpose convolutional layers to upsample the features and reconstruct the image.

The CNN model must then be trained using the original phantom data with the complete range of angles after being defined. In order to reduce the difference between the reconstructed images and the phantom in the ground truth, the model parameters are optimized during the training phase. The model weights are iteratively updated using the optimizer Adam with a learning rate value of 0.001 and a loss function which is the Mean Squared Error (MSE). To ensure convergence, the loss is tracked while the model is trained across 10000 of epochs.

Once our CNN model is trained, it can be used for image reconstruction. The sinogram data are preprocessed and normalized before being fed into the trained model. The model performs a forward pass, generating reconstructed images based on the input sinogram. The reconstructed images can then be visualized and evaluated.

VI. Results

A. ***Experiment 1***

In *Figure 5*, we can observe the reconstructed images constructed by MR-FBP for all four types of phantoms. In *Table I*, the mean absolute pixel error is shown so that we can understand that MR-FBP has a better performance on grayscale phantoms like the first one or the brain-like which is, also, grayscale, despite the noise added to it. On the other hand, it finds it more difficult to accurately reconstruct the binary phantom which is something we did not expect. This is maybe due to the limited contrast. In a black-and-white image,

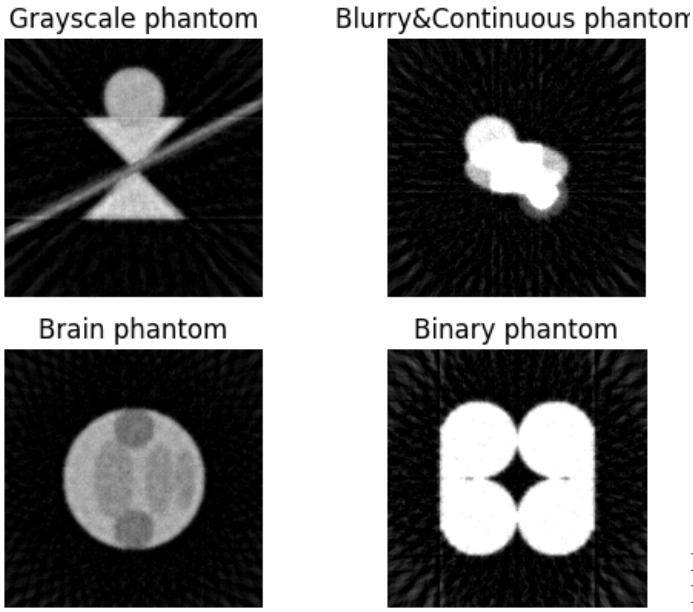

Fig. 5: Phantom Reconstruction by MR-FBP. Each phantom represents one different type of phantom: grayscale, blurry/Continuous, Brain-like, and Binary phantom.

there are only two intensity levels and this limited range of intensity values provides less contrast compared to a grayscale image that has a wide range of intensity values. The lack of contrast can make it challenging for the reconstruction algorithm to differentiate between different features or structures in the image. Also, this limitation to the intensity level makes it more sensitive to noise (we can indeed observe that in Figure 5). Moreover, a black-and-white image often contains sparse information, and the absence of fine details or variations in intensity can make it harder for the reconstruction algorithm to accurately capture the underlying structure of the image. The reconstruction of the continuous phantom seems to be more difficult than grayscale phantoms as well, and this can be caused by its complexity and the addition of noise.

However, the usage of the algorithm is very simple and user-friendly and the overall performance is relatively good, giving accurate enough reconstructions (based on the error metric) even though, in all phantoms, some artifacts are present.

TABLE I: Mean Absolute Pixel Errors

Phantom Type	Mean Absolute Pixel Error
Grayscale	0.055
Blurry & Continuous	0.077
Brain	0.058
Binary	0.096

B. Experiment 2

Here, we present the comparisons between MR-FBP with algorithms that are computationally less expensive but sacrifice accuracy like FBP, with algorithms that cost more like SIRT and CGLS and ones that try to compromise between cost and accuracy, like SIRT.

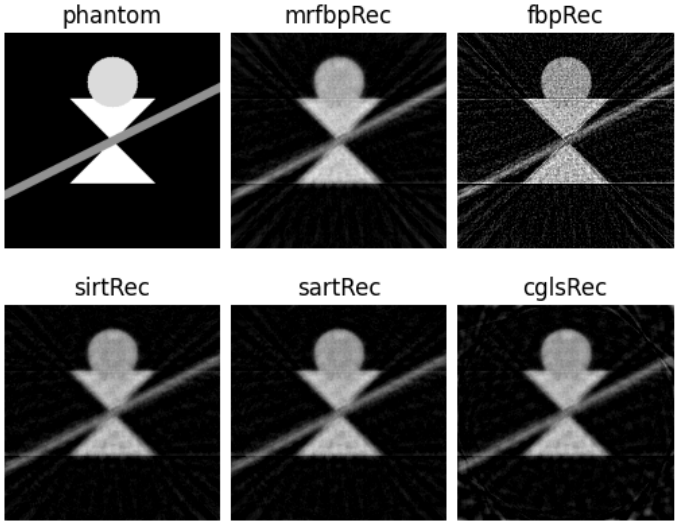

Fig. 6: Performance of the five algorithms on the grayscale Phantom.

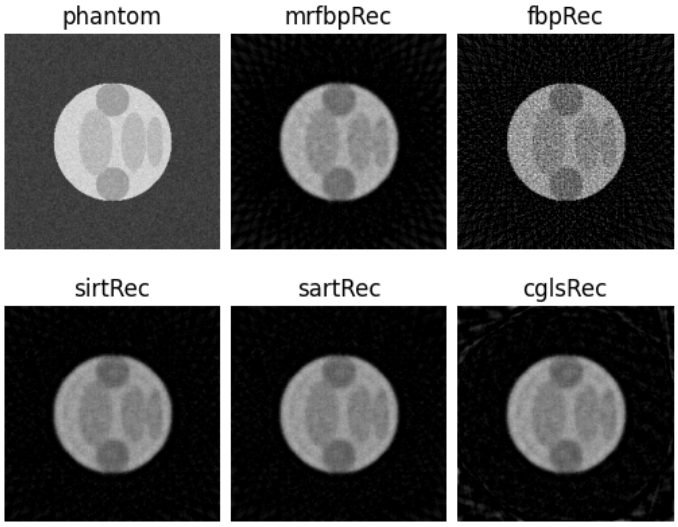

Fig. 7: Performance of the five algorithms on the brain-like phantom.

In *Figures 6-9*, the performance of all the algorithms, as well as MR-FBP, is shown for the four phantoms. Again, the mean absolute pixel errors are presentes in *Table II*, so as to discuss and compare the results based on the specific metric.

TABLE II: Mean Absolute Pixel Errors for Different Algorithms and Phantoms.

Phantom	**MR-FBP**	**FBP**	**SIRT**	**SART**	**CGLS**
Grayscale	0.056	0.140	0.049	**0.048**	0.059
Brain	0.058	0.119	**0.051**	**0.051**	0.059
Binary	0.097	0.241	0.075	**0.073**	0.105
Continuous	0.078	0.234	**0.070**	0.071	0.100

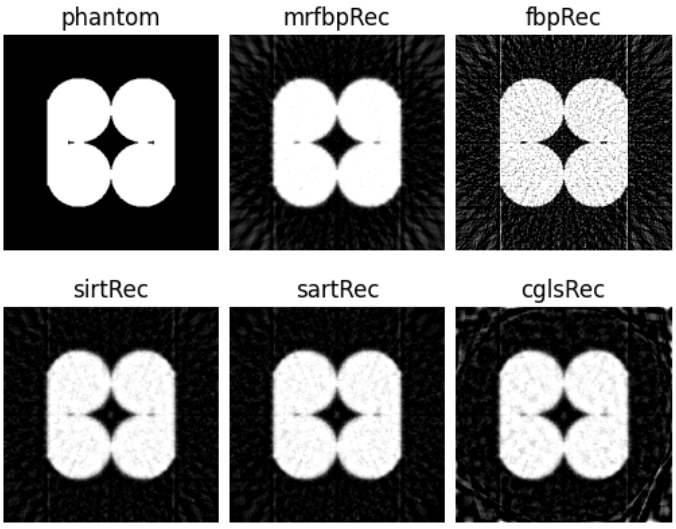

Fig. 8: Performance of the five algorithms on the binary phantom

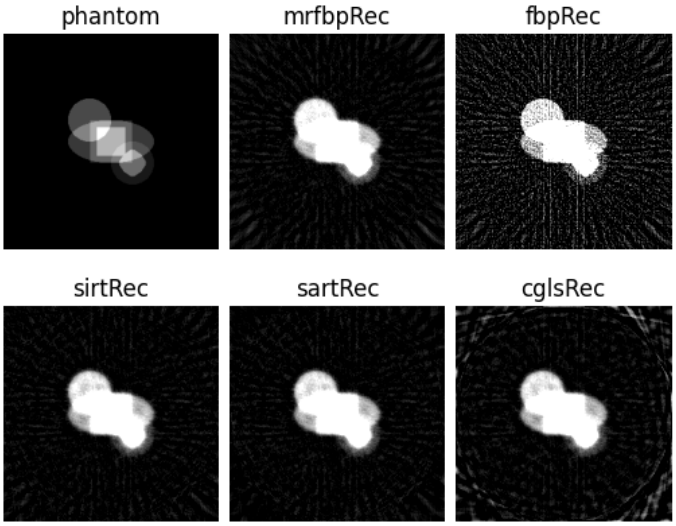

Fig. 9: Performance of the five algorithms on the blurry and continuous phantom.

We can observe that MR-FBP might not outperform all the other algorithms for any type of phantom, although its performance, based on the mean absolute pixel error, is not much worse, especially for the grayscale phantoms. Its performance on the brain-like phantom is surprisingly good, so we can say that in clinical cases could be useful to save computational time as its accuracy is competitive with SIRT and SART. Overall, even though MR-FBP does not give the best reconstructions, it appears to be really competitive with SIRT and SART, which give the best reconstructions, and if someone cares more about the computational time and cost, then MR-FBP is surely more suitable. In addition, there are many cases, like continuous or binary phantoms, where more complex and computationally expensive algorithms such as CGLS perform much worse than MR-FBP. Of course, it performs always better than FBP as we can say that MR-FBP is "an improvement" of FBP.

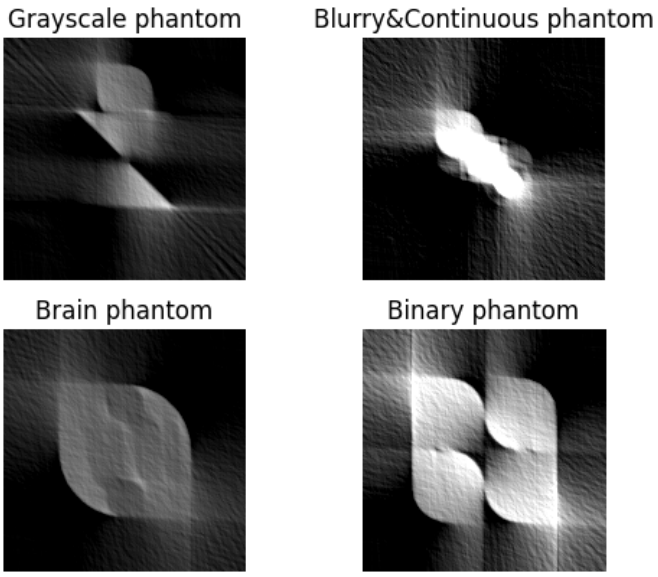

Fig. 10: MR-FBP performance on all four phantoms with angle range $[0,\pi/2]$.

C. *Experiment 3*

In the previous experiments, we were presenting the results using a full range of angles $[0,\pi]$. However, if reducing this range the results appear to be really damaged. We can get an idea of how our phantoms look like when using a range of $[0,\pi/2]$ (even though with a lot of artifacts) but as we keep tightening this range, we are no longer able to recognize not even the overall structure of the phantoms.

You can observe the reconstructed images by MR-FBP in *Figure 10* for the range $[0,\pi/2]$, *Figure 11* for the range $[0,\pi/4]$, and *Figure 12* for the range $[0,\pi/8]$.

We can conclude that MR-FBP is affected a lot by angle limitation so it might not be the more suitable method to use when the experimental setup and equipment do not permit using the full range of angles.

After getting these bad results we thought of reducing the complexity by disabling the addition of noise to the sinogram when the angle range is limited and examining if this could be helpful. So, with this, we move forward to Experiment 4 for the results.

D. *Experiment 4*

After disabling the addition of noise to the sinograms before the reconstruction when dealing with limited noise we got the reconstructed images that are presented in *Figure 13*. As you can observe, there is no significant improvement which is, also, expressed by the mean absolute pixel error which might be reduced by 0.01 or even less.

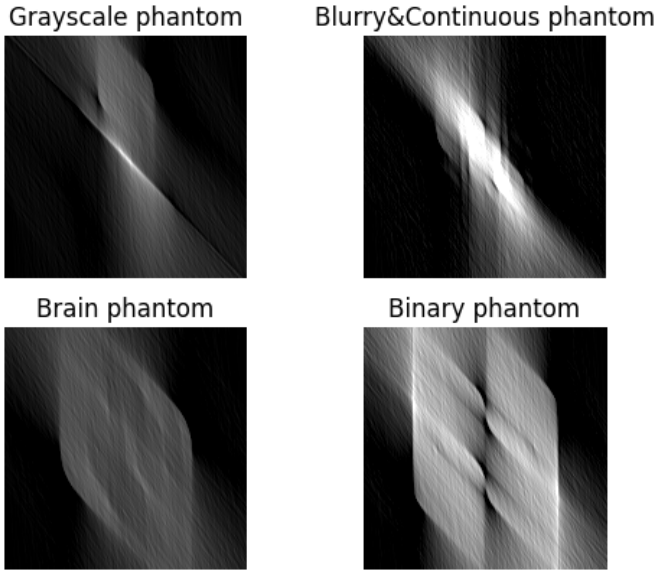

Fig. 11: MR-FBP performance on all four phantoms with angle range [0,$\pi/4$].

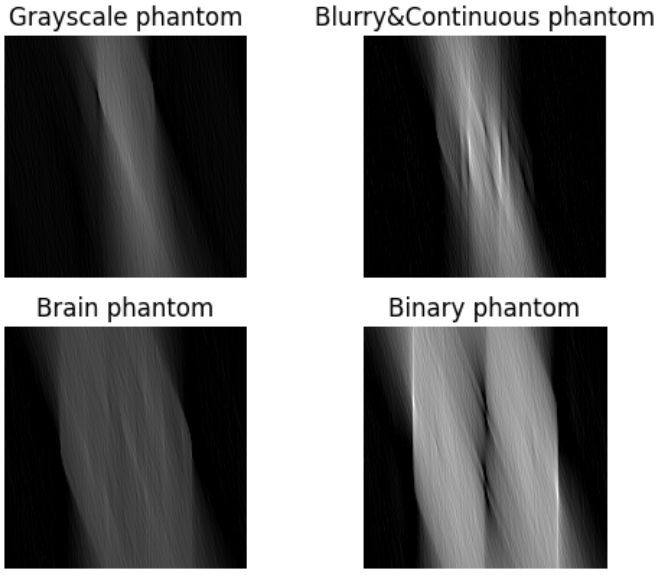

Fig. 12: MR-FBP performance on all four phantoms with angle range [0,$\pi/8$].

E. ***Experiment 5***

Finally, as we found some limitations of the MR-FBP, especially with angle limitations, we thought of comparing its performance with neural networks, and here are the results.

In *Figures 14-15*, you can observe the reconstructions for all the phantoms by the CNN. Figure 14 shows the reconstructions when using a full angle range, and the loss achieved by the network after 10000 epochs for each phantom is presented in *Table III*. Accordingly, in Figure 15 you can observe the same but now using an angle range of [0,π/4]. Again, the loss is

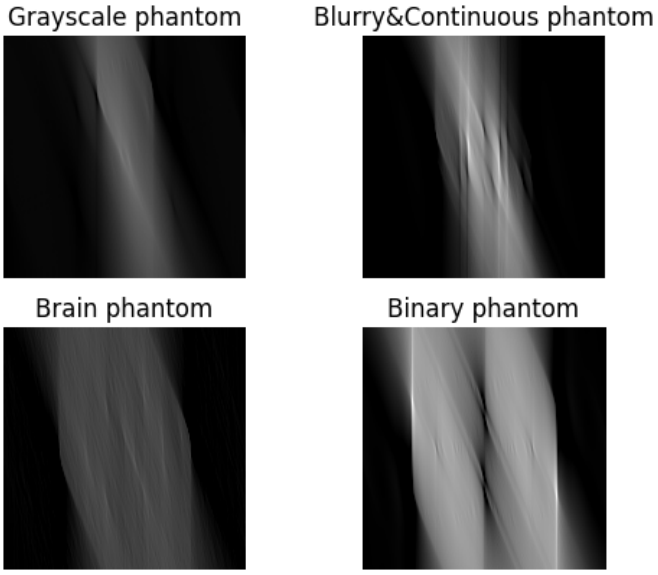

Fig. 13: MR-FBP reconstructions with limited angle range [0,π/8 without the addition of noise to the sinogram.]

shown in *Table III*.

In general, CNN performs much better than MR-FBP when dealing with limited angles. However, it is important to mention that our CNN trained and tested on the same phantoms to have these results. When the CNN is trained and tested on different phantoms we have really bad results as shown in *Figure 16*. Since our CNN was trained on a small sample size of data, this is to be expected, yet, it seems to be promising for future work. So, MR-FBP could be more desirable in cases where time and cost are important and, also, there are no limitations in the angle range but if it is impossible to use a full angle range or at least half of it, then CNN is required as MR-FBP can no longer be helpful.

Of course, if we observe the reconstructed images by CNN, we can see some weird artifacts, some lines that disturb the image. This may be caused by limited training. Also, this can be reduced by a better hyperparameter tuning like the learning rate. We did examine the effect of the learning rate and indeed it affects the presence of these lines. Maybe, some other loss functions, optimizers, and better overall tuning can really decrease the artifacts concluding in much more high-quality reconstructions.

Overall, about the deep learning approach, when trained to each specific phantom we get the results shown in Figures 14-15 which show a promising performance, giving reconstructions with higher quality than MR-FBP. However, if we consider training the CNN on a specific type of phantom and then using the trained model on another, new type of phantom, the results are really bad. So, in this case, the MR-FBP method is preferred. So, here we understand the complexity of a CNN and the multiple requirements that it has, making us think that sacrificing some accuracy by using our method MR-FBP is desirable.

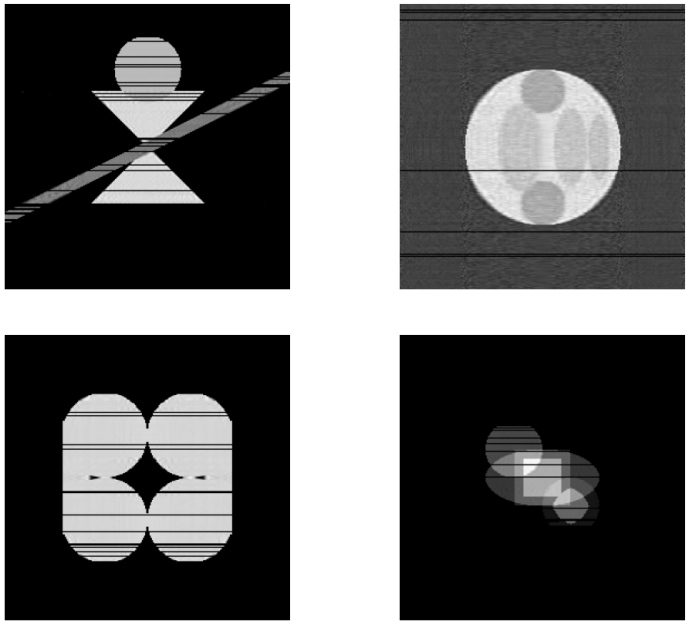

Fig. 14: Reconstructions of the four phantoms with full angle range [0,π] using CNN.

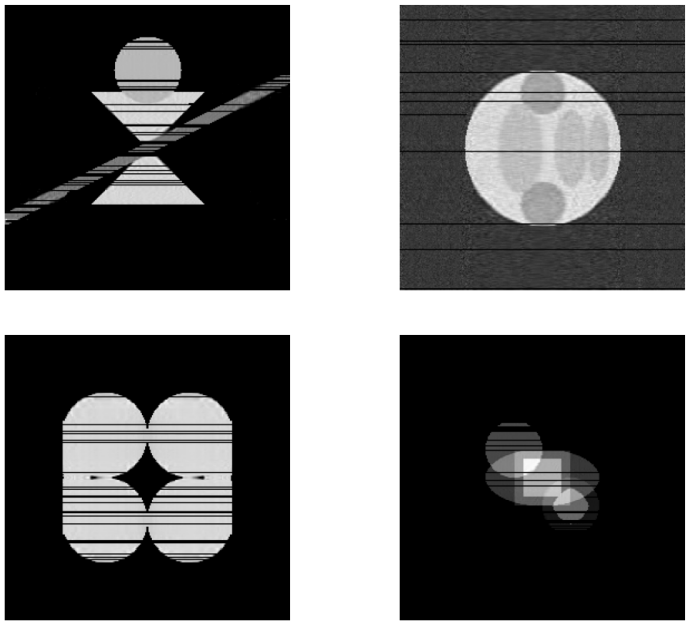

Fig. 15: Reconstructions of the four phantoms with limited angle range [0,π/4] using CNN.

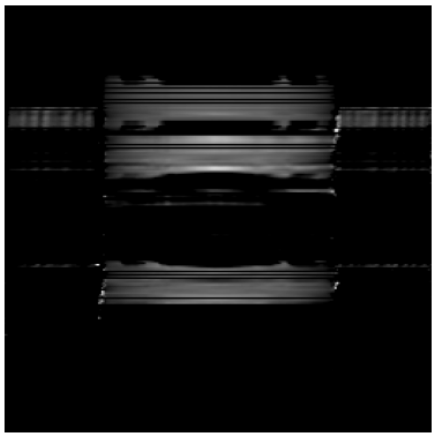

Fig. 16: Reconstruction of Brain phantom with full angle range using pre-trained CNN.

TABLE III: Loss for Different Angle Ranges and Different Phantoms using CNN

Phantom	Full Angle Range	Limited Angle Range
Grayscale	0.013	0.019
Brain	0.005	0.007
Binary	0.027	0.044
Continuous	0.002	0.002

VII. Discussion and conclusions

To sum up, the aim of this project is to evaluate the performance of the MR-FBP method, examine how it corresponds under certain circumstances when the environment is not ideal, investigate its competence with already existing algorithms easily provided by the ASTRA toolbox, and finally, compare it with a deep learning approach, a CNN and conclude in scenarios where MR-FBP is preferable and where it is not.

Observing our experiments one by one, we can say that from Experiment 1, we come to the conclusion that MR-FBP performs better in terms of reconstruction quality with grayscale images even if they include some noise like the brain phantom. However, when dealing with more complex images such as continuous or blurry images, it gives slightly worse results but still satisfying. The unexpected observation that we should not skip mentioning is its difficulty in reconstructing binary phantoms as it seems that the absence of details and intensities do not help the algorithm.

From Experiment 2, we learned that although there exist algorithms like SIRT and SART that perform better in all of the cases we examined, the divergence is not so big making the MR-FBP method competitive. Also, compared to algorithms like FBP and CGLS, our algorithm performs much better without increased complexity. Eventually, in scenarios when we can sacrifice slightly the accuracy of the image reconstruction, MR-FBP could be more desirable than all the other algorithms that we implemented in this paper.

However, here comes the limitations of the MR-FBP to show up, as Experiment 3 showed us that in scenarios when we cannot calculate projections from a full angle range, the

algorithm performs badly. We might be able to tighten the angle range at [0, π/2] but not more than that because then the reconstructions cannot even be representative. Even if we disable the addition of noise on the sinogram before the reconstruction, as we did in Experiment 4, the results are still poor.

Finally, through our deep learning approach, we considered more preferable to use a CNN rather than MR-FBP algorithm when dealing with angle limitations but CNN indeed has a lot of requirements. Neural networks might be computationally expensive and need a lot of training, maybe even a different training for each type of image. And even with that, it might not perform well on unknown images. So, in simpler situations, for example, when working with grayscale images and full angle range, MR-FBP can be more useful and satisfactory.

Overall, working with the ASTRA plugin that offers the MR-FBP algorithm is extremely easy and useful. The MR-FBP is built in a very smart way so as to be simple, not very time-consuming, and to give high-quality images when working with structures that are easier to be captured (like grayscale phantoms) and when the environment permits using full angle range for projecting the object. In more difficult situations, MR-FBP finds some difficulties and more complex methods like CNNs might be more preferable although demanding.

REFERENCES

[1] Daniel M. Pelt and Kees Joost Batenburg. *Improving Filtered Backprojection Reconstruction by Data-Dependent Filtering*.

[2] Ahn, J. (2018). *UNet: Line by Line Explanation*. Towards Data Science. Retrieved from https://towardsdatascience.com/unet-line-by-line-explanation-9b191c76baf5

[3] W. van Aarle, W. J. Palenstijn, J. Cant, E. Janssens, F. Bleichrodt, A. Dabravolski, J. De Beenhouwer, K. J. Batenburg, and J. Sijbers, "Fast and Flexible X-ray Tomography Using the ASTRA Toolbox", *Optics Express*, 24(22), 25129-25147, (2016). http://dx.doi.org/10.1364/OE.24.025129

[4] W. van Aarle, W. J. Palenstijn, J. De Beenhouwer, T. Altantzis, S. Bals, K. J. Batenburg, and J. Sijbers, "The ASTRA Toolbox: A platform for advanced algorithm development in electron tomography", *Ultramicroscopy*, 157, 35-47, (2015). http://dx.doi.org/10.1016/j.ultramic.2015.05.002

[5] W. J. Palenstijn, K. J. Batenburg, and J. Sijbers, "Performance improvements for iterative electron tomography reconstruction using graphics processing units (GPUs)", *Journal of Structural Biology*, vol. 176, issue 2, pp. 250-253, 2011. http://dx.doi.org/10.1016/j.jsb.2011.07.017